Boron evaporation in thermally-driven seawater desalination: Effect of temperature and operating conditions

A. Alpatova, A. Alsaadi, N. Ghaffour*

King Abdullah University of Science and Technology (KAUST), Water Desalination and Reuse Center (WDRC),
Biological and Environmental Science and Engineering Division (BESE), Thuwal 23955-6900, Saudi Arabia
*Corresponding author: noreddine.ghaffour@kaust.edu.sa

Abstract

The volatilization of boron in thermal desalination processes, namely multi-stage flash (MSF) and air-gap membrane distillation (AGMD) was investigated for the first time. This phenomenon was observed at feed temperatures above 55°C in both studied processes. In simulated MSF process with two feeds, model boric acid and Red Sea water, boron concentration in distillate increased with feed temperature increase from 55°C to 104°C because of the increase in boric acid vapor pressure. Salinity and pH were the main factors controlling boron evaporation. The achieved boron concentrations in simulated MSF process were consistent with those measured in distillate samples collected from commercial MSF plants. The AGMD process also revealed a strong influence of operating temperature on boron removal. However, unlike MSF process, the boron concentration in AGMD permeate decreased with the feed temperature increase from 55°C to 80°C due probably to increase in vapor production and corresponding permeate dilution. When AGMD was operated in concentrating mode at a constant feed temperature of 80°C, permeate boron concentration increased with process time due to concentration polarization and membrane fouling. A 10% flux decline observed after 21 h was attributed to $CaCO_3$ scaling on the membrane surface.

Keywords: Boron volatilization; Boron rejection; Seawater desalination; Multi-stage flush (MSF), Air gap membrane distillation (AGMD).

1. Introduction and background

Boron is a transitional element between the metals and non-metals, and at concentrations below 22 mg/L, the predominant boron forms are boric acid [H_3BO_3] (predominates in acidic

conditions) and borate ion [B(OH)$_4$$^-$] (predominates in alkaline conditions) [1]. The increase in temperature and salinity shifts the reaction equilibrium of boric acid – borate ion system towards formation of borate ions [2-4].

Boric acid is volatile at elevated temperatures according to the following equation [5]:

$$H_3BO_3(s) = H_3BO_3(g) \tag{1}$$

where (s) and (g) denote solid and gaseous phases of boric acid, respectively.

Brandani et al. [6] observed increase in vapor pressure over boric acid solutions with temperature increase concluding that evaporation of boron from boric acid solutions followed Henry's law. In a later study, Dickson et al. [3] investigated the combined effect of temperature and salinity on the boric acid – borate ion equilibrium and reported that at any given temperature, the values of equilibrium constants increased with salinity increase.

The variability of permissible boron concentrations in treated waters is based on health and environmental implications, boron occurrence and distribution in drinking water supplies, agricultural activities, and cost-efficiency of treatment technologies [7]. In general, countries which rely on freshwater as a major drinking water supply (e.g., USA, Canada), have more flexible boron regulations as comparing to those which use seawater desalination for drinking and irrigation purposes (e.g., Saudi Arabia) (Table 1).

Although the optimal boron concentration in irrigation water is in the range of 0.3 – 0.5 mg/L to ensure safe plant cultivation, some plants require lower boron concentrations to alleviate possible adverse effects [8]. The situation is more complicated in the arid and semi-arid areas of Middle East and Northern Africa (MENA) where the reduced boron leaching from the soils due to low annual rainfalls would promote boron accumulation in soils and may elevate boron uptake by the plants and crops [9].

Boron removal by thermal desalination

Over the past decades, seawater desalination has become a reliable and, in many cases, solitary technology of the freshwater production in countries which experience severe shortage of conventional water sources [10]. This encourages local authorities to extend the traditional thermal-based desalination technologies like multi-stage flush (MSF) and multi-effect distillation (MED), as well as augment the water supply by seawater reverse osmosis (SWRO), or by developing methods which combine membrane separation and thermal processes, e.g.,

membrane distillation (MD). The MD process is based on the transport of water vapor through the micro-porous hydrophobic membranes due to transmembrane temperature difference [11]. Since the water vapor is the only component which is transported through the membrane, high rejections of ions, low molecular weight organics and colloids can be achieved [12, 13]. MD does not require an intensive pre-treatment and offers better product quality compared to SWRO [14-17]. Another advantage of the MD technology is its lower heating regime as opposite to thermal evaporation where top brine temperature reaches 110ºC [18-20].

Due to variable boron drinking water standards across the world, it is important to ensure stringent freshwater quality. Depending on operating parameters, concentration of total dissolved solids (TDS) in the distillate from the thermal evaporation plants vary in the range of 5 – 50 mg/L [21], with Saudi Arabia setting a maximum TDS of 25 mg/L [22]. Khawaji et al. [18] emphasized that MSF plants could face constrains when brine droplets from flashing chambers are carried over with the vapor stream due to problems with the demister design, performance or its location within the evaporator, or inappropriate selection of anti-foaming agents. Moreover, due to extensive evaporation, the brine TDS is progressively increasing as brine is passing through flashing chambers which number could reach as high as 30 units [23]. As such, brine droplets, enriched with different seawater constituents, may enter condensing trays and reduce distillate quality. The existing research pertaining seawater desalination by conventional thermal evaporation reveals that neither boron volatility nor its distribution in distillate across the MSF stages as well as its overall removal efficiency and mechanisms remain a major research gap which has not been yet addressed.

Several studies investigated boron removal by the direct contact membrane distillation (DCMD), an MD process in which condensed vapor is continuously diluted into large volume of coolant solution [19, 20, 24, 25]. Therefore, the concentration of boron in permeate is expected to be low due to the dilution effect. Hou et al. [24] reported high boron rejections (>99.8%) from model solutions with the boron concentrations up to 1,500 mg/L. In a follow up study [19], the authors found that concentration of boron in permeates was below 10 µg/L at low concentration factors (CF), but started increasing with further CF increase. Similarly to these studies, Boubakri et al. [20] observed the boron rejection was above 90% at 200 mg/L of feed boron concentration. When seawater was used as a feed, boron concentration in permeate reached 0.47 mg/L after 18 h of operation. Wen et al. [25] investigated the effect of inorganic salts addition on boron

removal from radioactive water spiked with up to 5,000 mg/L of boron. The authors reported that at 300 mg/L of $NaNO_3$, permeate boron concentration was less than 2 mg/L. However, the real boron removal values of all these studies are questionable due to consecutive dilution of the coolant water by condensed water vapor in DCMD where permeate is mixed with coolant. As such, the actual amounts of boron transferred through the membrane in DCMD process can be higher than the reported ones. Moreover, due to different operating parameters and lower corresponding fluxes, the boron removal patterns by other MD configurations can be quite different from those reported for DCMD.

In recent years, air gap MD (AGMD) configuration is being rapidly developed. In this process the vapor condensation is achieved within the air gap created between a condensation surface and the membrane while the coolant stream flows on the other side of the condensation surface [26]. The collected AGMD permeate is then a condensed pure water vapor. Furthermore, the low thermal conductivity of air promotes decrease in the heat conduction from the membrane feed side to condensation side [27]. The elimination of the dilution factor allows not only for accurate estimation of the amount of boron transferred to the permeate site from the feed solution, but also for elucidation of the boron removal mechanisms with respect to water matrices and operating conditions. To the best of our knowledge, no research has been reported up to date with respect to boron evaporation (removal) in AGMD and MSF. In the literature, boron removal efficiency has been studied by other technologies only, such as reverse osmosis, ion exchange and electrocoagulation [28].

The aims of this study were to fill the existing research gaps with respect to boron volatility in thermal-based desalination processes, namely MSF and AGMD, and to conduct a comprehensive study on evaluating the efficiency of boron removal by these processes under different operating conditions and water matrices and elucidating corresponding boron removal mechanisms.

To simulate MSF evaporation process, seawater was boiled at temperatures corresponding to different vapor pressures in a range of 55ºC – 104ºC. The effect of pH on process efficiency was studied by conducting evaporation experiments in a pH range of 8.1 – 12.0 with boric acid solution at boron concentration corresponding to that of the Red Sea water. The quality of the distillate samples was than compared to that of distillate samples collected at different stages of commercial MSF plants located in the Red Sea and Gulf coasts.

We further determined the feasibility of boron removal by the AGMD process and investigated effect of operating conditions and solution chemistry on process performance and boron rejections. Firstly, we evaluated the effect of feed temperature in the range of 55°C – 80°C on boron transport and water vapor flux. This was followed by estimating the effect of process time and feed concentration on boron removal and membrane fouling in a continuous AGMD process at a feed temperature of 80°C. To investigate the effect of salinity on process performance, the water vapor flux and quality data from real seawater AGMD were compared with those obtained during AGMD process with boric acid solution under the same conditions.

The results of this study are expected to extend the existing knowledge with respect to removal of environmentally-relevant boron contaminant during water treatment and desalination, and aid in development of safe drinking water technologies.

2. Materials and methods

2.1. Waters

The MSF feed and distillate samples were supplied from three MSF facilities in Saudi Arabia (Plants 1 and 2 located on the Red Sea coast and Plant 3 located on the Arabian Gulf coast). The physico-chemical characteristics of these waters are shown in Table 2. Boric acid (H_3BO_3) solution with boron concentration of 5.55 mg/L was prepared by dissolving the appropriate amount of H_3BO_3 powder in Milli-Q water. The pH of solution was adjusted to 8.1 with 0.2 M NaOH by using the CyberScan 600 pH meter (EUTECH Instruments, Singapore).

2.2. Bench-scale evaporation experiments

The evaporation experiments were conducted by using Rotovapor® R-210 (Flawil, Switzeland) system equipped with a Buchi V-700 vacuum pump. To cool down the water vapor, the condenser was connected to a Huber Mini Chiller (Huber, Offenburg, Germany) set at 9°C. The evaporation experiments were conducted at 55°C, 65°C, 75°C, 85°C, 90°C and 104°C boiling temperatures. A 100 g of distillate was collected for further analysis to match 40% brine recovery. All experiments were conducted in duplicates.

2.3. AGMD process

AGMD of the model boric acid solutions and Red Sea water was performed by using the experimental set up shown in Fig. 1. The red and blue lines correspond to the feed and coolant flow lines, respectively. The electric heater (Model C25P, ThermoScientific, Waltham, MA, USA) and chiller (LM series, VWR, Radnor, PA, USA) were employed to maintain the stable temperature of the feed and coolant, respectively. The mass of accumulated permeate was measured with an electric balance (Model ML 3002, Metter Toledo, Columbus, OH, USA) and logged into the system by using Labview software (National Instruments, Austin, TX, USA). A 0.22 μm porous polypropylene membrane (Sterlitech Corporation, Seattle, WA, USA) was used through the entire set of experiments. Volumetric coolant and feed flow rates were set at 15 and 60 L/h, respectively.

2.4. Analytical methods

Temperature and conductivity were measured by a Cond 3210 conductivity meter (WTW GmbH, Weilheim, Germany). Concentrations of B^{3+}, Na^+, Ca^{2+} and Mg^{2+} were measured by an ICP-MS (7500 Series, Agilent Technologies, Santa Clara, CA, USA). Concentrations of Cl^- and SO_4^{2-} ions were measured by a Dionex ICS-1600 Ion Chromatographer (Thermofisher Scientific, Waltham, MA, USA). Concentration of dissolved organic carbon (DOC) in the Red Sea water and total organic carbon (TOC) in the MSF feeds were measured by the Shimadzu Total Organic Carbon Analyzer (TOC-V CSH Model, Shimadzu Corporation, Japan). Membrane surface was observed with the field emission scanning electron microscopy (FE-SEM, Quanta 200 FEG System, FEI, OR, USA). A Fourier transform infrared (FT-IR) spectrometer (Spectrum 100 Model, Perkin Elmer, Shelton, CT, USA) with an attenuated total reflectance (ATR) accessory was used to study the surface functionality of membranes.

3. Results and discussion
3.1. Effect of solution chemistry on boron evaporation
3.1.1. Temperature effect

As seen in Fig. 2, concentration of boron in the distillate samples collected at different boiling temperatures gradually increased from 1.2 ± 0.2 to 48.2 ± 2.1 μg/L and from 2.1 ± 0.6 to 58.4 ± 5.2 μg/L with the boiling temperature increase from 55ºC to 104ºC for seawater and boric acid solution, respectively. No boron was detected below these temperatures suggesting that

boron volatilization starts at temperatures above 55°C. The increase in distillate boron concentrations with temperature increase confirmed earlier observations that boron transfer from aqueous phase into vapor occurred according to Henry's law through evaporation of boric acid molecules which possess its own vapor pressure [29, 30]. The low distillate boron concentrations measured in our study were consistent with those previously reported (<1 to 60 µg/L) [30-35] due to significantly lower vapor pressure of boric acid (0.042 kPa at 100°C [29]) as compared to that of water (101.32 kPa at 100°C [36]).

3.1.2. Ion strength effect

The boric acid – borate ion interactions as a function of temperature and salinity also affects boron distribution between the liquid and the vapor phases as well as final boron concentration in distillate. As seen in Fig. 2, two trends were observed with respect to boron concentration depending on boiling temperature and ionic contents: (1) boron concentrations in distillate samples from seawater evaporation were lower comparing to those obtained from evaporation of boric acid solution, and (2) boron concentrations in distillate samples from evaporation of boric acid solution tended to increase to a greater extent with the boiling temperature increase as compared to those from seawater distillates. These trends could be explained as follows. The increase in boiling temperature shifts the reaction equilibrium of boric acid – borate ion system towards formation of more borate ions [2-4]. As a result, less amount of boric acid will be converted into vapor, so boron concentration in distillate would decrease. The increase in salinity of the feed water will further shift the balance between the boric acid and borate ions towards formation of more borate ions. Therefore, even less amount of boric acid would be available for volatilization. Consistently, lower boron concentrations will be found in distillate samples from seawater evaporation as compared to those of boric acid solution. As boiling temperature increased, a combining effect of salinity and temperature is expected to have more profound effect on boric acid volatility due to enhanced conversion of boric acid to borate ions. Therefore, the difference between the boron concentrations measured in the distillates from boric acid solution and seawater would tend to increase with the temperature increase to a more extent.

3.2.3. pH effect

Given that equilibrium in boric acid – borate system depends on solution pH, it is important to evaluate the change in boron concentrations in distillate samples with pH change, especially at high boiling temperatures as it has been shown that distillate boron concentration significantly increased with the temperature increase.

As shown in Fig. A.1 (Appendix), boron concentrations significantly decreased from 58.4 ± 2.1 to 6.5 ± 0.7 µg/L with pH increase from 8.1 to 12.0. In standard conditions, estimated molar fraction of boric acid at the initial boron concentration of 5.55 mg/L decreased from 0.93 to 0.002 with the pH increase from 8.1 to 12.0, respectively (Table A.1, appendices). It is important to mention that the increase in feed pH decreases the boron rejection in the RO process due mainly to size exclusion [2], which is different than the case of evaporation concept, the range of concentration values is also quite different (mg/L *vs* µg/L). As such, boric acid evaporation in these conditions will be negligible due to a significant predominance of the borate ions. Due to decrease in boric acid concentration with increasing evaporation temperature, the inflection point of boric acid – borate ion equilibrium will be shifted towards lower pHs as evaporation temperature increases, and the amount of boric acid available for evaporation will further decrease. However, as shown in Fig. S1, appreciable boron concentrations were measured in the distillate samples at 104°C in the alkaline pH range. This could be explained in the following way. It is known that for the same solution, pH measured at the *in situ* temperature will be different from that measured at ambient temperature. Based on Eq. (A.1), we calculated *in situ* pH values of boric acid solutions at 104°C which corresponded to ambient pHs in a range of 8.1 – 12.0 (Table A.2). As seen in Table A.2, calculated *in situ* pH values were lower than corresponding ambient pH values. As a result, the molar fraction of boric acid in alkaline conditions at 104°C was higher than expected. Furthermore, since the vapor pressure of boric acid over boric acid solution increased with the temperature increase, more boric acid molecules would evaporate at 104°C as compared to lower temperatures. Taken together, the decrease in actual solution pH and vapor pressure increase will enhance evaporation of boric acid at higher temperatures in the alkaline pH range.

3.2.4. Comparison with the distillate samples collected from commercial MSF plants

We further compared the boron concentrations measured in distillate samples collected at different boiling temperatures with boron concentrations in distillate samples collected after

brine evaporation at different stages of commercial MSF Plants. As shown in Figs. 2 and A.2 (Appendix), boron concentrations measured in our study were in the same range with the distillates obtained from MSF Plants. Consistently with our results, the boron concentration in distillate samples from MSF Plant 1 increased with increasing the brine temperature, with the highest boron concentration observed in the distillate from stage 1 (MSF Plant 1) at the top brine temperature (the highest temperature in the system) of 122.7^{o}C. As opposite, no boron was detected in the distillate from the last stage of MSF Plant 3. Usually, the brine temperature at the last stage of a typical MSF Plant is 40°C [37]. As such, the absence of boron in this distillate sample implies that boron evaporation from aqueous solution starts at temperatures higher than brine temperature of the last MSF stage. This observation is well-supported by our experimental data where only 2.1 ± 0.6 µg/L of boron were measured during the bench-scale seawater distillation experiments at 55°C (Fig. 2). Although the distillate samples from MSF Plants 1, 2 and 3 complied with the local drinking water limit for boron (0.5 mg/L) [38], it can be noted that boron concentration of the mixed sample from Plant 2 was higher (39.18 µg/L) as compared to those measured in distillate samples from Plant 1. The observed difference is due to the dilution effect as the distillate produced in the stages operating at temperatures lower than 55°C does not contain boron, and may also be caused by changes in operating parameters between the two plants.

As shown in Table A.3, conductivity of samples from Plant 1 decreased from 27.2 µS/cm to 11.1 µS/cm only with the temperature increase from 96.0 ^{o}C to 122.7 ^{o}C. The observed conductivity decrease may be caused by the increase in water vapor flux at high temperatures and corresponding condensate dilution as well as the increase in brine concentration throughout the stages.

3.2. Boron rejection in AGMD process

3.2.1. Effect of feed temperature on water vapor flux

The effect of feed temperature on water vapor flux and boron rejection in the AGMD process were conducted in a feed temperature range of 65°C – 80°C and a constant coolant temperature of 18°C. As seen in Fig. 3, an increase in the feed temperature from 65 to 80 ^{o}C resulted in water vapor flux increase from 6.46 to 12.80 kg/m^{2}h (by 198%) and from 5.96 to 13.12 kg/m^{2}h (by 221%) for the seawater and boric acid solution, respectively. Pairwise comparison of water vapor

fluxes of two waters obtained at corresponding feed temperatures and data fitting (dashed lines in Fig. 3) showed that while no significant differences in water vapor fluxes between the two feeds were observed at 65°C and 70°C, water vapor flux from the boric acid solution increased to higher degree when the feed temperature was further increased to 80 $^{\circ}$C. In general, MD is less sensitive to feed water quality and concentration polarization as compared to other membrane processes [14-17, 39, 40]. However, concentration polarization became more distinct with the temperature increase due to increase in water vapor flux which promotes accumulation of salts near the membrane surface [41]. Similar to our results, Duong at al. [42] observed a decrease in water vapor flux as compared to the theoretically calculated ones during seawater AGMD. Scale formation potential of feed water which increases with feed temperature is another factor which may negatively affect water vapor flux [43]. It has been reported that the scale formed on membrane surfaces as a result of decreased salts solubility, reduces water vapor flux [43-45]. As such, a lower water vapor flux from seawater AGMD process at higher temperatures observed in our study could be attributed to a combined effect of concentration polarization and membrane fouling which was more pronounced at 80°C as compared to lower feed temperatures.

3.2.2. Effect of feed temperature on boron rejection and permeate quality

As shown in Fig. 4, permeate boron concentrations from seawater AGMD process were lower as compared to those obtained from boric acid solution at any tested feed temperature. As discussed previously, concentration of borate ions in solution increases with salinity increase. As a consequence, the lower vapor pressure of boric acid over the seawater would decrease the boric acid vapor flux through the membrane, causing a reduction in boron concentrations in seawater permeate.

While concentration of boron in permeate samples from boric acid AGMD process gradually decreased with the feed temperature increase, no significant changes were observed with respect to boron concentration in permeate samples from seawater AGMD process (Fig. 4). This phenomenon can be explained by dilution effect which is caused by the difference in water vapor pressures at different feed temperatures. As such, more water vapor will be transferred through the membrane at higher temperatures, and the transferred boric acid will be diluted in larger permeate volume. In other words, at constant boron rejection rate, boron concentration in permeate will be lower at higher feed temperatures because of the higher flux obtained under

these conditions. Consistently, the conductivity (or TDS) of permeate samples also increased with temperature decrease (Table A.4). In the case of seawater, a combined salinity and temperature effect will reduce the amount of boric acid available for evaporation at high temperatures as compared to low temperatures. Therefore, the observed effect will be less pronounced and boron concentration in permeates from seawater will be changed to a less degree as compared to boric acid.

By comparing data presented in Tables A.4 and A.5, it is very clear that physico-chemical characteristics of permeates are well-correlated with distillates produced by bench-scale distillation process not only with respect to boron concentrations, but also with respect to other physico-chemical parameters including conductivity and pH.

As it is also shown in Fig. 4, the boron rejections for both seawater and boric acid solutions were all above 99% at any tested feed temperature. The boron rejections in the AGMD process were superior comparing to those observed in our earlier study on seawater desalination by RO process even though we did not apply any pretreatment or pH adjustment [16]. Moreover, although this study confirmed the boron volatility in thermally-driven desalination processes operating at high temperatures ($>55^{\circ}C$), the permeate boron concentrations were significantly below local stringent boron drinking water standard (0.5 mg/L) and for other applications, such as agriculture [46, 47]. The observed results suggest great potential of AGMD process in rejecting contaminants which are difficult to remove during conventional treatment because of their sensitivity to pH and salinity changes.

3.2.3. Effect of concentrating mode on water vapor flux and boron rejection

As shown in Fig. 5, different water vapor flux patterns were observed for the seawater and boric acid solution feeds at different process times. While water vapor flux of boric acid solution was higher and did not change with time (13.2 and 13.1 kg/m^2h at 0 and 21 h, respectively), a 10% decrease in water vapor flux after 21 h of operation was observed when seawater was used as feed (12.8 and 11.5 kg/m^2h at 0 and 21 h, respectively). Because this set of experiments was conducted in concentrating mode, the feed salinity would increase with time due to continuous permeate production. At the same time, the feed heating will cause rapid shift in system's bicarbonate-carbonate equilibrium towards formation of more carbonate ions. As such, the solubility limits of the scale-causing salts will be reached faster, and the scale will deposit on the

membrane surface. As reported in Table A.6, the conductivity of permeate increased with the process time, indicating membrane pore wetting due to scaling. A similar effect was observed by Duong et al. [42] during seawater AGMD process.

Our observations are supported by the surface composition analysis of the virgin and fouled membranes. As seen in Fig. 6, in contrast to a clean and smooth surface of a virgin membrane (Fig. 6a), a scattered crystal deposition was observed on the surface of fouled membrane which was subjected to 21 h of AGMD operation at 80°C (Fig. 6b). A close investigation of the crystal morphology revealed that it was predominated by the flower-like structures. The flower-like crystals are characteristic of the aragonite polymorph of $CaCO_3$ which is formed in solution at temperatures above 70°C [48]. Consistently, a follow up ATR FT-IR analysis of the fouled membrane revealed new peaks at 853 and 753 cm^{-1} (Fig. A.1), which were also attributed to $CaCO_3$ deposition on membrane surface [49] common for feeds with high saturation indexes [50]. Importantly, surface of fouled membrane was not fully covered with the scale deposits, and a considerable part of pores was still open to vapor transfer. This observation is in a good correlation with the water vapor flux data (Fig. 5) which showed that the water vapor flux decreased by only 10% even after 21 h of operation.

As shown in Fig. 7, concentration of boron in permeates increased with time for both tested solutions. Since the feed was continuously concentrating, it is expected that the concentration polarization will cause accumulation of boric acid near the membrane surface. As such, the boric acid vapor flux would increase and permeate will be enriched with the boric acid. This result is consistent with the observations of Boubakri et al. [20] and Wen et al. [25] who reported an increase in permeate boron concentration with the increase in boron feed concentration during the DCMD processes with model boric acid solutions. Additionally, Francis et al. [13] reported a boron concentration of 30 µg/L in DCMD permeate using Red Sea water as feed.

As expected, boron concentrations in permeate when AGMD process was conducted with boric acid feed solution were higher compared to that of seawater. A higher salinity of the feed water in the case of seawater AGMD process promoted the accumulation of borate ions near the membrane surface which, in turn, reduced the boric acid vapor flux through the membrane. The increase in membrane fouling, on the other hand, excerpted a negative effect on the boric acid vapor flux due to scale formation. As such, less boric acid was transferred through the membrane

in this case. As shown in Fig. 7, the boron rejections from both feed solutions were above 99% and did not significantly depend on the feed water recovery.

Conclusions

In the bench-scale evaporation process, boron concentration in distillates increased with the temperature increase due to increase in boric acid vapor pressure. Salinity and pH were found to be the main factors controlling boron evaporation at any given temperature. Permeate boron concentrations during AGMD decreased with the temperature increase due to increase in water vapor production and corresponding permeate dilutions. In concentrating mode experiments at 80 ºC, boron concentrations in permeates increased with the process time because of the increase of feed concentration and membrane scaling. A 10% flux decline observed after 21 h of AGMD operation was attributed to $CaCO_3$ deposition on the membrane surface.

Acknowledgement

## References

[1] K.L. Tu, L.D. Nghiem, A.R. Chivas, Boron removal by reverse osmosis membranes in seawater desalination applications, Separation and Purification Technology, 75 (2010) 87-101.
[2] R.E. Zeebe, A. Sanyal, J.D. Ortiz, D.A. Wolf-Gladrow, A theoretical study of the kinetics of the boric acid–borate equilibrium in seawater, Marine Chemistry, 73 (2001) 113-124.
[3] A.G. Dickson, Thermodynamics of the dissociation of boric acid in synthetic seawater from 273.15 to 318.15 K, Deep Sea Research Part A. Oceanographic Research Papers, 37 (1990) 755-766.
[4] I. Hansson, A new set of acidity constants for carbonic acid and boric acid in sea water, Deep Sea Research and Oceanographic Abstracts, 20 (1973) 461-478.
[5] R. Balasubramanian, T.S. Lakshmi Narasimhan, R. Viswanathan, S. Nalini, Investigation of the vaporization of boric acid by transpiration thermogravimetry and Knudsen effusion mass spectrometry, The Journal of Physical Chemistry B, 112 (2008) 13873-13884.
[6] V. Brandani, G. Del Re, G. Di Giacomo, Thermodynamics of aqueous solutions of boric acid, Journal of Solution Chemistry, 17 (1988) 429-434.

[7] N. Hilal, G.J. Kim, C. Somerfield, Boron removal from saline water: A comprehensive review, Desalination, 273 (2011) 23-35.

[8] P.P. Power, W.G. Woods, The chemistry of boron and its speciation in plants, Plant and Soil, 193 (1997) 1-13.

[9] R. Reid, Can we really increase yields by making crop plants tolerant to boron toxicity?, Plant Science, 178 (2010) 9-11.

[10] N. Ghaffour, The challenge of capacity building strategies and perspectives for desalination for sustainable water use in MENA, Desalination and Water Treatment, 5 (2009) 48-53.

[11] E. Curcio, G.D. Profio, E. Fontananova, E. Drioli, 13 - Membrane technologies for seawater desalination and brackish water treatment, in: Advances in Membrane Technologies for Water Treatment, Woodhead Publishing, Oxford, 2015, pp. 411-441.

[12] P. Wang, T.-S. Chung, Recent advances in membrane distillation processes: Membrane development, configuration design and application exploring, Journal of Membrane Science, 474 (2015) 39-56.

[13] L. Francis, N. Ghaffour, A.S. Alsaadi, S.P. Nunes, G.L. Amy, Performance evaluation of the DCMD desalination process under bench scale and large scale module operating conditions, Journal of Membrane Science, 455 (2014) 103-112.

[14] E. Drioli, A. Ali, F. Macedonio, Membrane distillation: Recent developments and perspectives, Desalination, 356 (2015) 56-84.

[15] J. Koschikowski, M. Wieghaus, M. Rommel, V.S. Ortin, B.P. Suarez, J.R. Betancort Rodríguez, Experimental investigations on solar driven stand-alone membrane distillation systems for remote areas, Desalination, 248 (2009) 125-131.

[16] K. Rahmawati, N. Ghaffour, C. Aubry, G.L. Amy, Boron removal efficiency from Red Sea water using different SWRO/BWRO membranes, Journal of Membrane Science, 423–424 (2012) 522-529.

[17] J. Redondo, M. Busch, J.-P. De Witte, Boron removal from seawater using FILMTEC high rejection SWRO membranes, Desalination, 156 (2003) 229-238.

[18] A.D. Khawaji, I.K. Kutubkhanah, J.-M. Wie, Advances in seawater desalination technologies, Desalination, 221 (2008) 47-69.

[19] D. Hou, G. Dai, J. Wang, H. Fan, Z. Luan, C. Fu, Boron removal and desalination from seawater by PVDF flat-sheet membrane through direct contact membrane distillation, Desalination, 326 (2013) 115-124.

[20] A. Boubakri, S.A.-T. Bouguecha, I. Dhaouadi, A. Hafiane, Effect of operating parameters on boron removal from seawater using membrane distillation process, Desalination, 373 (2015) 86-93.

[21] C.S. Bandi, R. Uppaluri, A. Kumar, Global optimization of MSF seawater desalination processes, Desalination, 394 (2016) 30-43.

[22] N.A. Nada, A. Zahrani, B. Ericsson, Experience on pre- and post-treatment from sea water desalination plants in Saudi Arabia, Desalination, 66 (1987) 303-318.

[23] S.-H. Choi, On the brine re-utilization of a multi-stage flashing (MSF) desalination plant, Desalination, 398 (2016) 64-76.

[24] D. Hou, J. Wang, X. Sun, Z. Luan, C. Zhao, X. Ren, Boron removal from aqueous solution by direct contact membrane distillation, Journal of Hazardous Materials, 177 (2010) 613-619.

[25] X. Wen, F. Li, X. Zhao, Removal of nuclides and boron from highly saline radioactive wastewater by direct contact membrane distillation, Desalination, 394 (2016) 101-107.

[26] A. Alkhudhiri, N. Darwish, N. Hilal, Treatment of high salinity solutions: Application of air gap membrane distillation, Desalination, 287 (2012) 55-60.

[27] M. Khayet, T. Matsuura, Membrane Distillation: Principles and Application, Elsevier, The Netherlands, 2011.

[28] B. Zeboudji, N. Drouiche, H. Lounici, N. Mameri, N. Ghaffour, The influence of parameters affecting boron removal by electrocoagulation process, Separation Science and Technology, 48 (2013) 1280-1288.

[29] S. Bezzi, Gazzetta Chimica Italiana, 65 (1935) 766.

[30] M.V. Stackelberg, F. Quatram, J. Dressel, Die Fluchtigkkeit der Borsauren mit Wasserdampf, Z. Elektrochem, 43 (1937) 14.

[31] M. Nishimura, K. Tanaka, Sea water may not be a source of boron in the atmosphere, Journal of Geophysical Research, 77 (1972) 5239-5242.

[32] Y.K. Xiao, S.Z. Li, H.Z. Wei, A.D. Sun, W.G. Liu, W.J. Zhou, Z.Q. Zhao, C.Q. Liu, G.H. Swihart, Boron isotopic fractionation during seawater evaporation, Marine Chemistry, 103 (2007) 382-392.

[33] J.A. Gast, T.G. Thompson, Evaporation of boric acid from sea water, Tellus, 11 (1959) 344-347.

[34] E.F. Rose-Koga, S.M.F. Sheppard, M. Chaussidon, J. Carignan, Boron isotopic composition of atmospheric precipitations and liquid–vapour fractionations, Geochimica et Cosmochimica Acta, 70 (2006) 1603-1615.

[35] B. Chetelat, J. Gaillardet, R. Freydier, P. Négrel, Boron isotopes in precipitation: Experimental constraints and field evidence from French Guiana, Earth and Planetary Science Letters, 235 (2005) 16-30.

[36] L. Haar, J.S. Gallagher, G.S. Kell, NBS/NRC Steam Tables, Hemisphere Publishing Corp., New York, 1984.

[37] H.T. El-Dessouky, H.M. Ettouney, Fundamentals of Salt Water Desalination, Elsevier Science, Amsterdam, 2002.

[38] Saudi Arabia Standards, Metrology and Quality Organization, Botted water standard. http://www.saso.gov.sa/en/standards/Pages/default.aspx (accessed 26.04.2017).

[39] J. Xu, Y.B. Singh, G.L. Amy, N. Ghaffour, Effect of operating parameters and membrane characteristics on air gap membrane distillation performance for the treatment of highly saline water, Journal of Membrane Science, 512 (2016) 73-82.

[40] A. Alsaadi, L. Francis, H. Maab, G. Amy, N. Ghaffour, Evaluation of air gap membrane distillation process running under sub-atmospheric conditions: Experimental and simulation studies, Journal of Membrane Science, 489 (2015) 73-80.

[41] A.L. Zydney, Stagnant film model for concentration polarization in membrane systems, Journal of Membrane Science, 130 (1997) 275-281.

[42] H.C. Duong, M. Duke, S. Gray, P. Cooper, L.D. Nghiem, Membrane scaling and prevention techniques during seawater desalination by air gap membrane distillation, Desalination, 397 (2016) 92-100.

[43] M. Gryta, Alkaline scaling in the membrane distillation process, Desalination, 228 (2008) 128-134.

[44] E. Curcio, X. Ji, G. Di Profio, A.O. Sulaiman, E. Fontananova, E. Drioli, Membrane distillation operated at high seawater concentration factors: Role of the membrane on CaCO3 scaling in presence of humic acid, Journal of Membrane Science, 346 (2010) 263-269.

[45] P. Zhang, P. Knötig, S. Gray, M. Duke, Scale reduction and cleaning techniques during direct contact membrane distillation of seawater reverse osmosis brine, Desalination, 374 (2015) 20-30.

[46] Y. Gacem, S. Taleb, A. Ramdani, S. Senadjki, N. Ghaffour, Physical and chemical assessment of MSF distillate and SWRO product for drinking purpose, Desalination, 290 (2012) 107-114.

[47] T. Sutton, U. Baumann, J. Hayes, N.C. Collins, B.-J. Shi, T. Schnurbusch, A. Hay, G. Mayo, M. Pallotta, M. Tester, P. Langridge, Boron-toxicity tolerance in barley arising from efflux transporter amplification, Science, 318 (2007) 1446-1449.

[48] H. Wang, V. Alfredsson, J. Tropsch, R. Ettl, T. Nylander, Formation of CaCO3 Deposits on Hard Surfaces—Effect of Bulk Solution Conditions and Surface Properties, ACS Applied Materials & Interfaces, 5 (2013) 4035-4045.

[49] M.G. Lioliou, C.A. Paraskeva, P.G. Koutsoukos, A.C. Payatakes, Heterogeneous nucleation and growth of calcium carbonate on calcite and quartz, Journal of Colloid and Interface Science, 308 (2007) 421-428.

[50] F.A. Miller, C.H. Wilkins, Infrared Spectra and Characteristic Frequencies of Inorganic Ions, Analytical Chemistry, 24 (1952) 1253-1294.
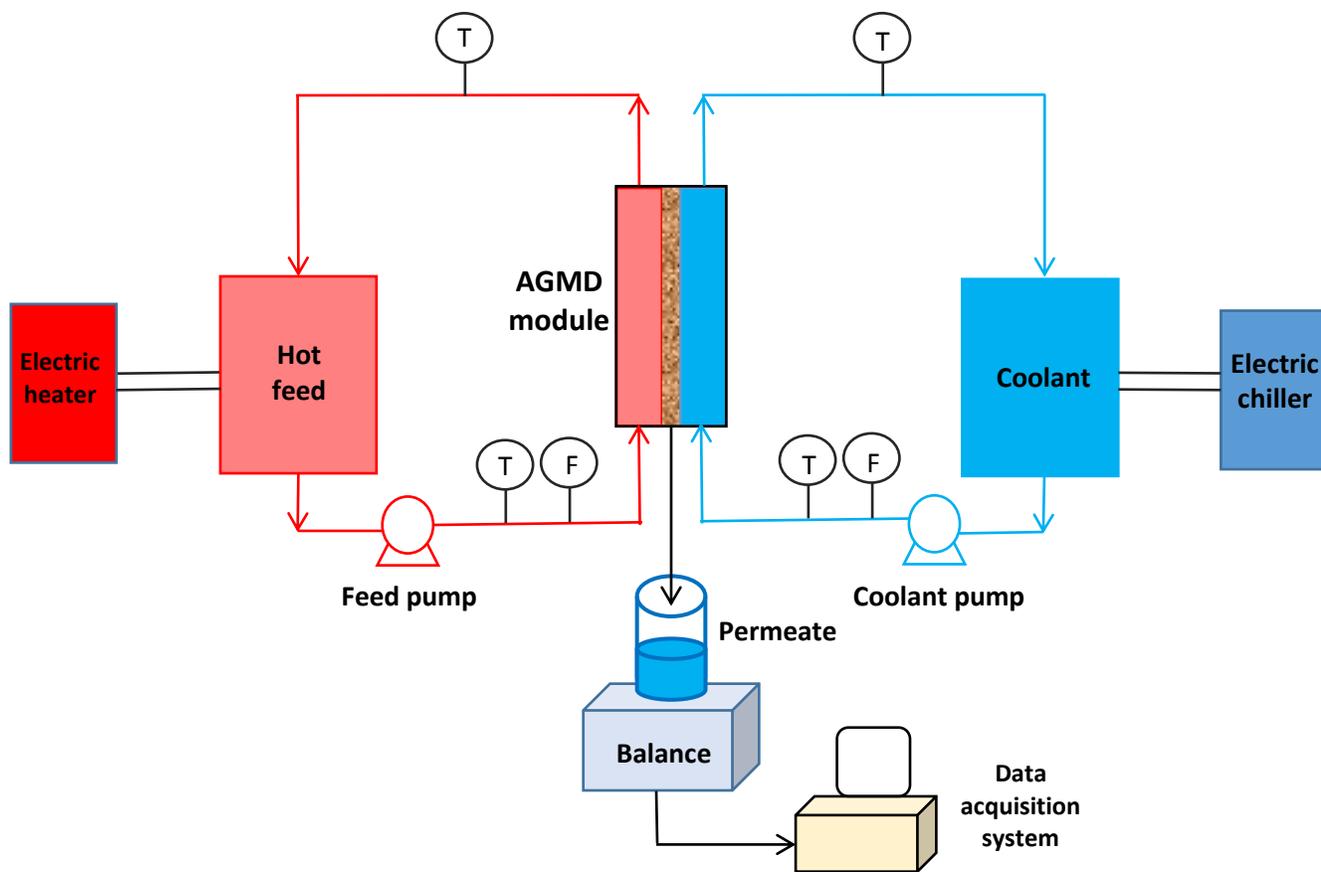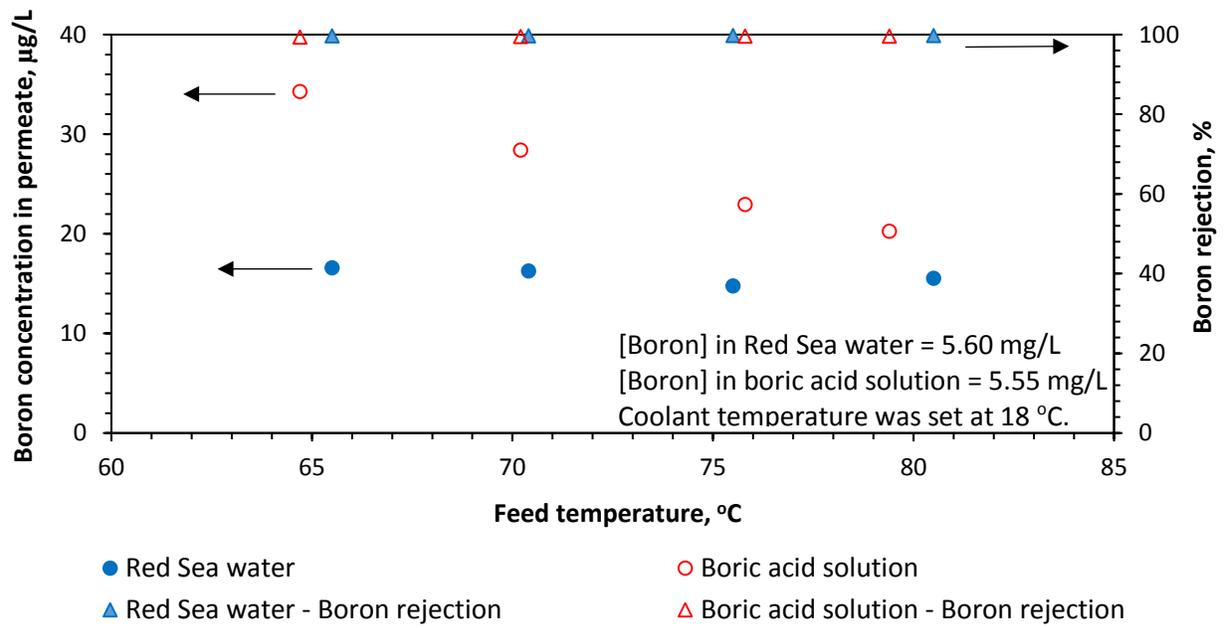
**Figure 1.** Schematic of the AGMD process.
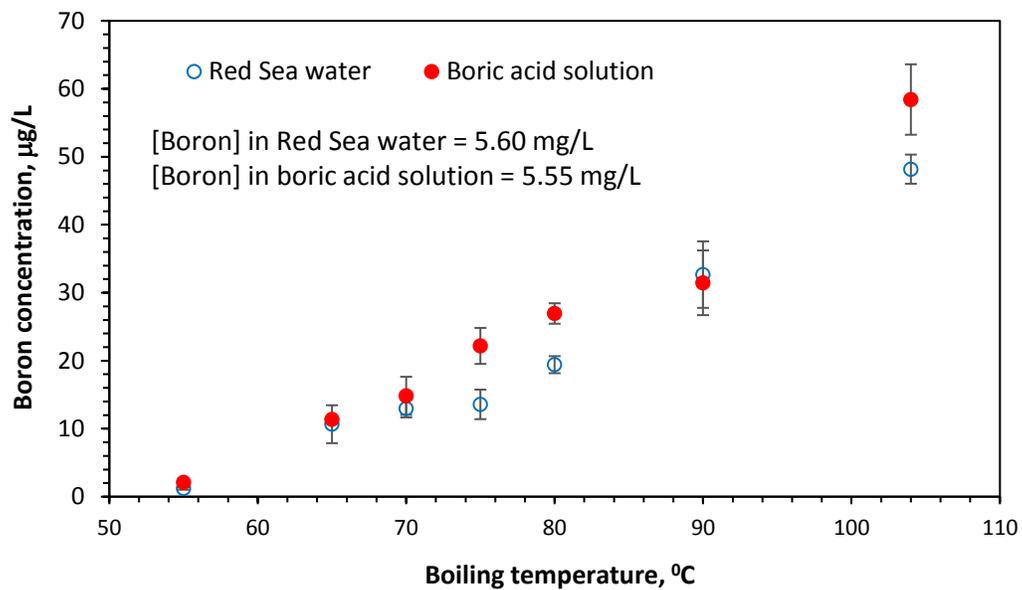
Figure 2. Boron concentration in distillate samples from evaporation of Red Sea water and boric acid solution at different boiling temperatures.
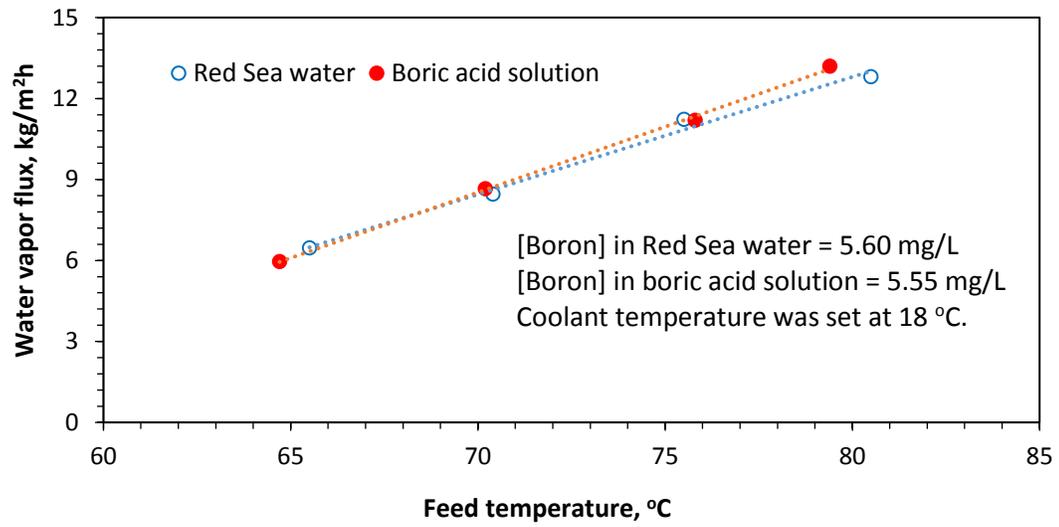
Figure 3. Water vapor flux (J_W) during AGMD process at different feed temperatures for the Red Sea water and boric acid solution.
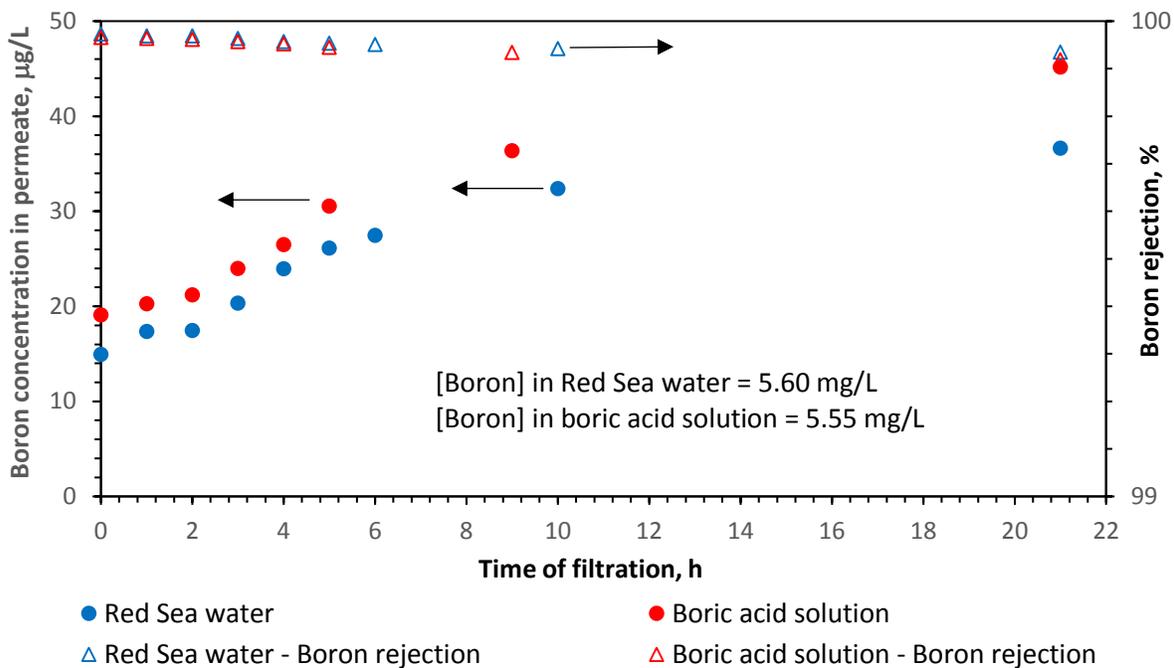
Figure 4. Boron concentration in AGMD permeates (circles) and boron rejection (triangles) at different feed temperatures for the Red Sea water and boric acid solution.
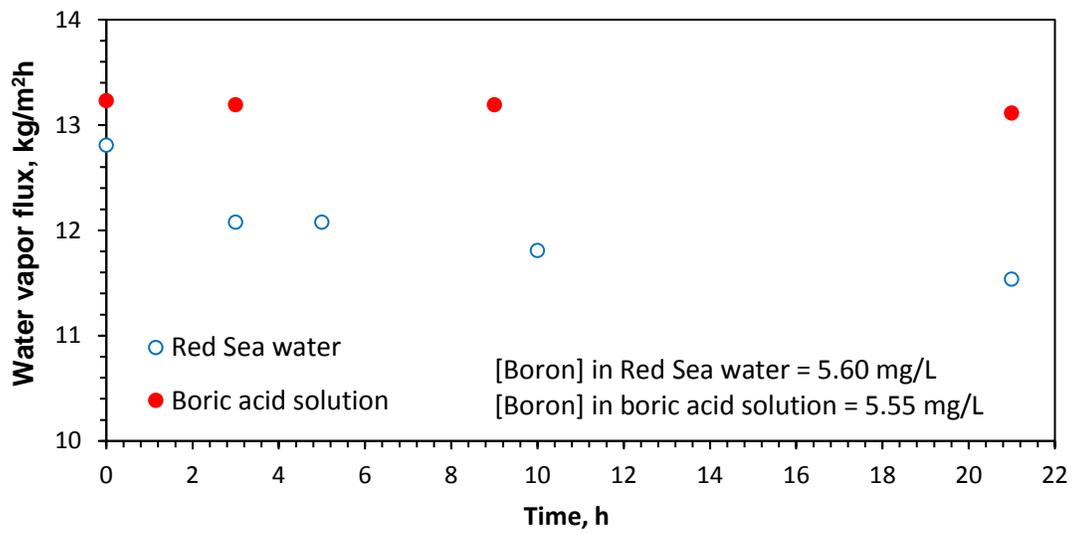
Figure 5. AGMD water vapor flux (J_W) vs time for the Red Sea water and boric acid solution. Coolant and feed temperatures were set at 18 and 80°C, respectively.
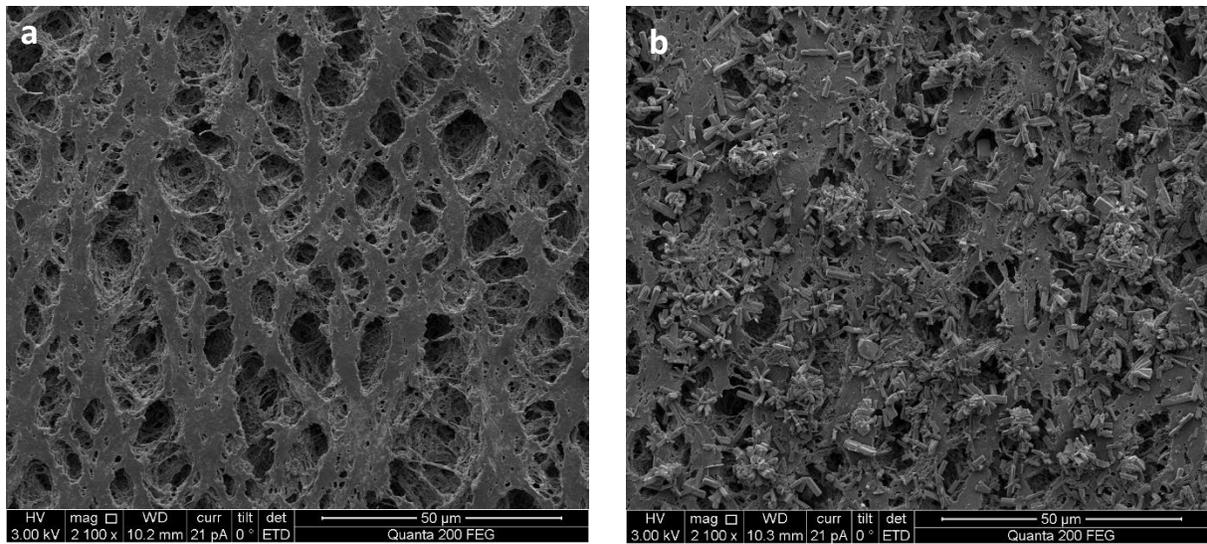
Figure 6. SEM images of the top surface of polypropylene membrane: (a) virgin membrane and (b) fouled membrane after 21 h of seawater AGMD process.

Figure 7. Concentration of boron in AGMD permeates (closed circles) and boron rejection (open triangles) at different process times for the Red Sea water and boric acid solution. Coolant and feed temperatures were set at 18ºC and 80ºC, respectively.